Temperature Dependence of the Behavior of an Epoxy−Amine System near the Gel Point through Viscoelastic Study. 1. Low-T_g Epoxy−Amine System

J. P. Eloundou,[†,§] M. Feve,[†] J. F. Gerard,[*,†] D. Harran,[‡] and J. P. Pascault[†]

Laboratoire des Matériaux Macromoléculaires, URA CNRS 5627, Institut National des Sciences Appliquées de Lyon, 20, Avenue Albert Einstein, 69 621 Villeurbanne Cedex, France, and Laboratoire de Physique des Matériaux Industriels, Centre Universitaire de Recherche Scientifique, Avenue de l'Université, 64 000 Pau, France

Received February 21, 1996; Revised Manuscript Received June 20, 1996[⊗]

ABSTRACT: A flexible epoxy−amine system based on the diglycidyl ether of 1,4-butanediol (DGEBD) and 4,9-dioxa-1,12-dodecanediamine (4D) was studied between 40 and 70 °C by rheological and viscosimetric methods near the gel point. This temperature domain is located well above the maximum glass transition temperature of the fully cured network, for which $T_{g\infty} = -12$ °C. At the gel point, the theoretical extent of reaction, x_{gel}, is equal to 0.5745, considering the reactivity ratio, n, of the secondary amines to the primary ones equal to 1.1 (equireactivity, $n = 1$). For the times corresponding to x_{gel}, the rheological curves follow a classical behavior, i.e., (i) divergence of the viscosity in steady flow conditions, (ii) crossover of the tan δ curves measured as a function of time at several frequencies, and (iii) proportionality between G' and G'' and the pulsation ω^{Δ} ($G'(\omega)$ and $G''(\omega)$ are proportional to ω^{Δ}). Above 50 °C, the exponent, Δ, is constant and equal to the average value of 0.70 ± 0.02. The width of the relaxation time spectrum is evaluated by studying the fully cured network. The highest value of Δ observed at low temperatures (40 °C) can be explained assuming that, in such a case, the longer relaxation times become similar to the observation times. Close to the gel point, the power laws $\eta \propto$ to ϵ^{-k} and $G' \propto \epsilon^{z}$ (where $\epsilon = |x - x_{gel}|/x_{gel}$), which govern the viscosity, η, and the elastic modulus, G', are verified within a large domain. The exponent k is constant with the temperature and is equal to 1.44 ± 0.03. The log G' vs $f(\log \epsilon)$ curves display two linear domains, at least for low temperatures and high frequencies. In the second domain, the exponent z varies with frequency, but above 50 °C, its value of $\omega = 1$ rad/s remains constant with the temperature ($z_0 = 2.65 \pm 0.02$). The values of exponents k, z_0, and Δ are in good agreement with those obtained from the percolation theory with molecular chains obeying the Rouse model.

Introduction

Recently, many authors have studied theoretically[1−6] and experimentally[7−28] the rheological behavior of chemicals and physical gels. Some mechanical properties, such as steady state shear viscosity, η, and equilibrium shear modulus, G, vary as power laws in the vicinity of the gel point. For example, at the gel point, the complex shear modulus, G^*, follows a power law of angular frequency, ω. These works appear as practical applications of percolation theories.[29−33]

The aim of this work is to look at the temperature dependence of the chemorheological behavior of epoxy−amine systems near the gel point by means of viscoelastic measurements.

In the first part, a low-T_g epoxy−amine system based on the diglycidyl ether of 1,4-butanediol (DGEBD) and 4,9-dioxa-1,12-dodecanediamine (4D) was chosen. The maximum glass transition temperature of the fully cured network of this system is low ($T_{g\infty} = -12$ °C), and its chemical kinetics is well known.[34] The temperature domain under study is well above $T_{g\infty}$; thus, in this temperature range, the reactive system displays only gelation.

In the second part, a high-T_g epoxy−amine system with a maximum glass transition temperature $T_{g\infty} =$ 177 °C will be considered below and above $T_{g\infty}$. In this case, the reactive system can display both gelation and vitrification.

Background

The percolation model[29−33] was developed to describe the properties of branched polymers near the gel point. In the bond percolation model, the monomers that occupy the sites of dimension, d, are randomly linked with the probability, x. When x is low, some dimers and trimers develop, and, as x increases progressively, larger clusters appear (branched polymers). For a critical value, x_{gel}, an infinite cluster appears, having a size and a mass that diverge at the gel point. Above x_{gel}, very large clusters connect together to give an infinite one, as a consequence, strengthening the network. The finite clusters with an average size decreasing as the reaction proceeds are included in these very large clusters. The structural parameters are related to each other by the following scaling laws:

(i) The size distribution of the clusters (number of clusters of mass m) is

$$N(m) \propto m^{-\tau} \exp(-m/M_z) \qquad (1)$$

where M_z is the z-average molar mass, which has the same critical behavior as the mass of the largest cluster before the gel point. Beyond the gel point, M_z is equivalent to the gel fraction, n_g.

* To whom correspondence should be addressed.
† Institut National des Sciences Appliquées de Lyon.
‡ Centre Universitaire de Recherche Scientifique.
§ Present address: Laboratoire de Mécanique des Matériaux et Constructions. Ecole Nationale Supérieure Polytechnique, BP 8390, Yaoundé (Cameroon).
⊗ Abstract published in *Advance ACS Abstracts,* August 15, 1996.

S0024-9297(96)00287-2 CCC: $12.00

(ii) The mass m is expressed as a function of the radius of gyration by

$$m \propto R^{d_f} \tag{2}$$

where d_f is the fractal dimension of the polymer. The radius, ξ, of M_z is called the correlation length.

Near the gel point, several quantities diverge as power laws of ϵ ($\epsilon = |x - x_{gel}|/x_{gel}$):

$$\xi \propto \epsilon^{-\nu} \tag{3}$$

$$M_z \propto \xi^{d_f} \propto \epsilon^{-1/\sigma} \tag{4}$$

Combining eqs 3 and 4 gives

$$d_f = 1/(\sigma\nu) \tag{5}$$

The dimensions d and d_f are associated by the hyperscaling law

$$d = d_f(\tau - 1) \tag{6}$$

Beyond the gel point, the gel fraction varies as

$$n_g \propto \epsilon^{\beta} \tag{7}$$

with

$$\beta = (\tau - 2)/\sigma \tag{8}$$

Three-dimensional simulations ($d = 3$) give $\tau = 2.2$, $d_f = 2.5$, and $\nu = 0.89$.

The mechanical properties, such as the viscosity, η, at zero frequency and the equilibrium modulus, G, also vary as power laws of ϵ:

$$\eta \propto \epsilon^{-k} \qquad \text{(before the gel point } x < x_{gel}) \tag{9}$$

$$G \propto \epsilon^{z} \qquad \text{(beyond the gel point } x > x_{gel}) \tag{10}$$

Considering the electrical analogy, η corresponds to the conductivity of a mixture of superconductors and conductors, and x_{gel} is the supraconduction threshold. G corresponds to the conduction of a mixture of conductors and insulators; x_{gel} is the conduction threshold. In this way, three-dimensional simulations lead to $k = 0.75 \pm 0.04$[29,30,32] and $z = 1.94 \pm 0.01$.[30,31]

In the Rouse model approach, the macromolecule is considered as a bead spring free of any hydrodynamic interaction with the solvent, which then can be of the same nature as the polymer. This approach can be applied to the case of a reaction proceeding in bulk. As a consequence, the viscosity is purely entropic and varies as the mass-average square of the radius of gyration, $\langle R^2 \rangle_w$.[29] The calculations made in this case lead to

$$\eta \propto M_z^{\,2-\tau+2/d_f} \propto \epsilon^{(2-\tau+2/d_f)/\sigma} \propto \epsilon^{\beta-2\nu} \tag{11}$$

In a three-dimensional percolation model, $k = \beta - 2\nu$; thus, $k = 1.33$.

Close to the gel point, eq 2 shows that the clusters forming the "polymolecular medium" are described in terms of fractal geometry. The fractal domain corresponds to scaling lengths which are included between the monomer size and the correlation length, ξ, which varies as the size of the largest cluster.[35] If the fractal dimension describes the way the object occupies the volume, however, it gives no indication on the connectivity. As a consequence, a spectral dimension, d_s, was introduced[1,2] which reflects connectivity and takes into account the diffusion as well as the transfer phenomena in the network. This spectral dimension is given by

$$N_t \propto t^{d_s/2} \tag{12}$$

where N_t is the number of distinct sites visited during a random walk in the network.

The number of steps executed is proportional to the time, t, of the random walk and is connected to the average radius, R_w, of the visited space by means of the fractal dimension of the random walk in the network:

$$t \propto R_w^{\,d_w} \tag{13}$$

The three dimensions d_f, d_s, and d_w verify the relation

$$d_s = 2d_f/d_w \tag{14}$$

By comparing the percolating system with a mixture of conductors and insulators beyond the gel point, one obtains[1]

$$d_s = 2d_f/[2 + (z - \beta)/\nu] \tag{15}$$

Alexander and Orbach[1] have observed, from various simulations, that the spectral dimension is always close to $^4/_3$ in the case of percolation with a space dimension, d, between 1 and 6. For $z = 1.94$ (three-dimensional percolation), the value 1.35 was found for d_s.

The existence of a fractal domain is expressed by a distribution of relaxation times, λ (time taken by a cluster to diffuse on a length equal to its own radius), from a lower limit, λ_0, to an upper limit, λ_z.[35] The upper limit does not take into account the divergence of the largest cluster size when approaching the gel point, and the lower limit takes into account the similarity loss for very small dimensions.

The viscoelastic measurements showed that, at the gel point, the distribution of relaxation times obeys a power law:[7−15]

$$H(\lambda)\, \mathrm{d} \ln \lambda \propto \lambda^{-\Delta}\, \mathrm{d} \ln \lambda \tag{16}$$

The shear relaxation modulus, which describes the relaxation strain proceeding from a constant shear deformation, can be obtained by[36]

$$G(t) = \int_0^{\infty} [H(\lambda)/\lambda]\, e^{-t/\tau}\, \mathrm{d}\lambda \propto t^{-\Delta} \qquad (\lambda_0 < t < \lambda_z) \tag{17}$$

Thus, by applying the Fourier transform to eq 17,[36]

$$G(\omega) \propto \omega^{\Delta} \qquad (1/\lambda_z < \omega < 1/\lambda_0) \tag{18}$$

It appears, then, that two limits exist: $\omega^* = 1/\lambda_z$ and $\omega_0 = 1/\lambda_0$, and between these values, G' and G'' vary according to a power law of ω:

$$G'(\omega) \propto G''(\omega) \propto \omega^{\Delta} \qquad (\omega^* < \omega < \omega_0) \tag{19}$$

The measurement frequencies are generally very low compared to ω_0, which corresponds to the monomer size. Generally, only ω^* is taken into account. Thus, as the frequency is lower than ω^*,[36] (i) before the gel point, the medium can be considered as a Newtonian liquid for which $G'(\omega)$ and $G''(\omega)$ are proportional to ω^2 and to ω, respectively; (ii) after the gel point, the medium is

Table 1. Experimental Values of Exponents *k*, *z*, and Δ

reaction	*k*	*z*	Δ
DGEBA[a]/Jeffamine D400 (D400), $T_{g\infty} = 35$ °C < T_i (70 < T_i < 100 °C)	1.3 ± 0.2[19]		0.72 ± 0.02[18] 0.70 ± 0.03[19]
DGEBA/diethanolamine (DEA), $T_{g\infty} = 70$ °C < $T_i = 90$ °C	1.4 ± 0.2[16,20,21]	2.8 ± 0.2[20]	0.70 ± 0.05[20,21]
DGEBA/4,4′-diaminodiphenyl sulfone (DDS), $T_{g\infty} = 200$ °C > $T_i = 90$ °C			0.63 ± 0.01[22]
hydrolysis and polycondensation of silyl-terminated poly(oxypropylene)	1.2 ± 0.2[23] 1.0 ± 0.1[24]	2.1 ± 0.1[23] 2.0 ± 0.1[24]	0.69 ± 0.02[23] 0.66 ± 0.02[24]
hydrolysis and polycondensation of alkoxysilane groups			0.63 ± 0.02[25]
hydrolysis and polycondensation of the tetraethoxysilane		2.4 ± 0.2[17] 2.49−5.24,[26] depending on pH	0.72 ± 0.02[17]
polycaprolactone + triisocyanate			0.3−0.83,[14,15] depending on molar ratio
poly(dimethylsiloxane) + silane			0.2−0.9,[9−13] depending on molar ratio
solution of gelatin in water (physical gel)		0.68−2.11,[26] depending on pH 1.9[28]	0.64−0.72,[27] depending on pH

[a] DGEBA = diglycidyl ether of the bisphenol A.

equivalent to an elastic solid for which G' is constant and $G''(\omega)$ is proportional to ω; and (iii) at the gel point, where an infinite macromolecule appears, ω^* tends toward zero. Using the Kronig−Kramers relations,[36]

$$G''/G' = \tan\delta = \tan(\pi\Delta/2) \tag{20}$$

Many authors[1−6] successfully connect the exponents Δ, k, z, σ, τ, and ν with the dimensions d, d_f, d_s, and d_w.

In the Rouse model, for which the hydrodynamic interactions are totally screened, the relaxation time, λ_i, of a cluster of mass, M', is proportional to M'.[17,35,37] The surroundings of a molecule of mass M are based on smaller fractals, which relax at times, λ_i. Thus, λ_i is lower than λ', which is proportional to M', and the larger clusters are considered immobile in the time scale of the testing.[6,16] The diffusion factor D_t ($D_t \propto R^2/\lambda$) is then inversely proportional to the mass. In the Zimm limit of the excluded volume, where the hydrodynamic interactions are strong, the diffusion factor is given by the Stokes−Einstein relation and varies as R^{2-d}. Martin et al.[6] showed that the exponent k must be between a lower limit (Zimm) and an upper limit (Rouse); thus,

$$0 < k < \nu(d_f + 2 - d) \tag{21}$$

As a consquence,

$$d/(d_f + 2) < \Delta < 1 \tag{22}$$

and as

$$\Delta = d\nu/(d\nu + k) \quad \text{and} \quad z = d\nu \tag{23}$$

$$\Delta = z/(z + k) \tag{24}$$

Restricting their approach to the Rouse model, Rubinstein et al.[5] proposed the following equations:

$$d_s = 2d_f/(d_f + 2) \tag{25}$$

$$k = 2/\sigma d_s - (\tau - 1)/\sigma \tag{26}$$

$$z = (\tau - 1)/\sigma \tag{27}$$

Considering eqs 5, 6, and 8, it can be shown that eqs 11, 21, and 26 are similar to eqs 23 and 27 and to the Rouse limit, respectively. In addition, eq 24 can be easily found from eqs 26 and 27. As a consequence, in a three-dimensional percolation, d_s, k, and z are found to be equal to 1.11, 1.33, and 2.67, respectively.

The expression $\Delta = d/(d_f + 2)$ was also established by Muthukumar,[2,3] who studied the dependence of the dynamic viscosity on the frequency ($\eta^* \propto \omega^{\Delta-1}$) in dense media, where the hydrodynamic interactions are completely screened (Rouse model). The value $d_s = 1.11$ found by Rubinstein et al.[5] is different from that presented by Alexander and Orbach[1] ($d_s = 1.33$). However, one notices that, if a value $z = 2.67$ is introduced in eq 12, $d_s = 1.11$ is obtained in the three-dimensional percolation. These two values of d_s lead to $\Delta = 0.67$. In the electrical analogy, eq 24 leads to $\Delta = 0.72$.

In the case of an ideal gel, where the cross-links are linked each other by "phantom chains" (i.e., there is no interaction with the adjoining chains), the elastic modulus is inversely proportional to the number, N, of units which constitute these chains ($G \propto kT/N$, where k is the Boltzman constant and T the absolute temperature). Each of these effective chains, included in a correlation volume ξ^d, constitutes a fractal cell of dimension d_f; thus, N and G are proportional to ξ^{d_f} and ξ^{-d_f}, respectively. Equation 13 leads to the following relation:

$$\omega \propto 1/t \propto R_w^{-d_w} \tag{28}$$

As a consequence,

$$G \propto \omega^{d_f/d_w} \propto \omega^{d_s/2} \tag{29}$$

For $d_s = 4/3$, $\Delta = 0.66$ ($d_s/2$).

For Martin et al.,[6] the modulus, which is purely entropic, is proportional to the density of the correlation blobs in the gel ($G \propto kT/\xi^d$). Equation 28 leads to

$$G \propto \omega^{d/d_w} \propto \omega^{(d_s/2)(d/d_f)} \tag{30}$$

Taking $d_s = 1.11$, a value for Δ of 0.67 ($= (dd_s)/(2d_f)$) is found in the three-dimensional percolation.

The approach developed by Martin et al.[6] seems more realistic. Equations 3, 10, and 23 lead to G proportional to ξ^{-d}. On the other hand, from eqs 5, 6, and 8,

$$d\nu = d_f\nu + \beta = 1/\sigma + \beta \tag{31}$$

Combining eq 31 with eqs 4, 7, 10, and 23,

$$G \propto kTn_g/M_z \tag{32}$$

In this way, it can be connected with the rubber elasticity theory, in which the elastic modulus is proportional to the density of the elastically active network chains.[38,39] The derivative of the logarithm of the complex modulus G^* varies as a power law[12,40] near the gel point:

$$\partial(\log G^*)/\partial x \propto \partial(\log G^*)/\partial t \propto \omega^{-\kappa} \quad (33)$$

The maximum relaxation time, λ_z, is expressed by

$$\lambda_z \propto \epsilon^{-(k+z)} = \epsilon^{-1/\kappa} \quad (34)$$

Thus, it can be seen that

$$k = (1 - \Delta)/\kappa \quad \text{and} \quad z = \Delta/\kappa \quad (35)$$

The literature gives $\kappa = 0.4$ for the electrical analogy and $\kappa = 0.25$ in the percolation theory (Rouse model). Experimental determination of the values of k, z, and Δ has been the subject of extensive studies. Some of these results are reported in Table 1.

Even if the values of these exponents depend on the considered systems, a good agreement with the percolation theory for epoxy−amine systems is observed. The lowest value of Δ found for the diglycidyl ether of bisphenol A (DGEBA)/4,4′-diaminodiphenyl sulfone (DDS) system[22] could be attributed to the curing temperature, which is lower than the maximum glass transition temperature, $T_{g\infty}$ (about 200 °C). The mobility conditions are, in this case, completely assumed since some molecular chains have long relaxation times, according to the broadness of the relaxation times spectrum. The values of z and Δ found for the physical gel of a solution of gelatin in water and for the chemical gel obtained by hydrolysis and polycondensation of poly(oxypropylene) silane are similar. Thus, a physical cross-linking obeys the same laws as the chemical gelation. For the condensation of various divinyl-terminated poly(dimethylsiloxane) with a tetrafunctional silane hardener, Scanlan and Winter[12] found $\kappa = 0.21$. This value remains constant as Δ varies with molar ration from 0.2 to 0.9.[9−13]

It can be noticed that the measurements of the storage shear modulus, G', are not performed at zero frequency. As a consequence, Yu and Amis[26] observed a dependence of z on the frequency used for the dynamic measurements. Furthermore, they distinguished two linear parts of the curve log G' vs log ϵ. This effect can be related to the fact that, at non zero frequency, an elastic response (i.e., a storage shear modulus, G') appears before the gel point. Thus, the change of the z exponent value might express the modification from a flexible network to a much more rigid network beyond the gel point.[26,41]

Experimental Part

Reagents. The diglycidyl ether of 1,4-butanediol (DGEBD) and the 4,9-dioxa-1,12-dodecane diamine (4D) from Aldrich were used as received. The values for the molar masses of the two monomers are close to each other (202.25 and 204.32 g, respectively), leading to a comparable length and flexibility for the chains between cross-links. The functionalities of DGEBD and 4D are 2 and 4, respectively. For a stoichiometric ratio of epoxy to amino hydrogens (e/a) equal to 1, the concentration of epoxy groups in the initial monomer mixture, e_0, is equal to 6689 mol/m^3. All measurements were done for a stoichiometric ratio e/a = 1.

Viscosimetry. The changes of the viscosity during the reaction of DGEBD and 4D was followed with a Searle Contraves Rheomat 115 type viscometer at a constant temperature from 40 to 70 °C. Above 70 °C, the gelation times are too short and the measurements are little reliable because of the time needed to reach a thermal equilibrium (in the kinetic study reported previously,[34] the measurements performed at 90 °C were not taken into account for the same reasons). During the measurement, the shear rate varies from 0.065 to 1000 s^{-1} as a function of the measured torque.

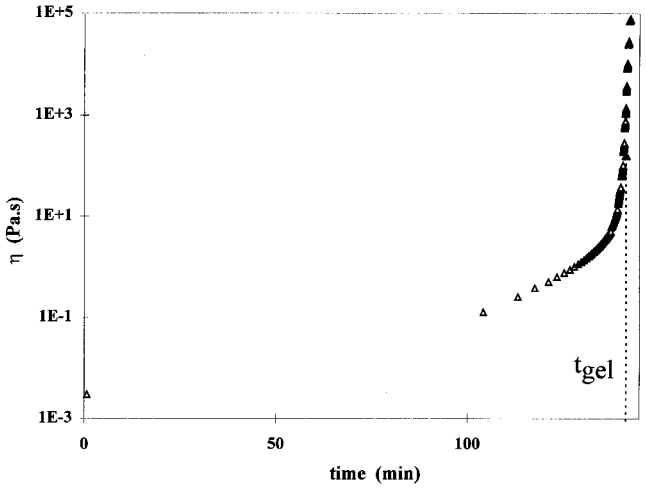

Figure 1. Experimental curve of viscosity η as a function of time, t, at 50 °C.

Table 2. Times (in Minutes) for Gelation of the DGEBD/4D System at Different Temperatures of Reaction

	T (°C)				
	40	50	55	60	70
$x = 0.5745$		143.5	98.2	76.8	38.8
$\eta = 1000$ Pa·s	293.7	141.3	102.5	76.9	39.3
crossover of tan δ	290.2	136.1	97.3	72.8	36.8
$G' \propto G'' \propto \omega^{\Delta}$	290.7	136.1	99.9	72.6	36.7
average value	291.5	139.3	98.2	74.8	37.9
discrepancy (%)	1	3	3	3	4

Dynamic Mechanical Measurements. The dynamic mechanical spectra of DGEBD/4D reactive system were recorded at constant temperature from 40 to 70 °C in a frequency range from 10 to 100 rad/s. A Rheometrics Dynamic Analyzer (RDA 700) apparatus equipped with a parallel plates tool was used in this study. The plates diameter and the thickness were 40 and 1.5 mm, respectively. The shear strain was fixed to 5%. Because of the very low viscosity in the initial monomer mixture and of the narrowness of the gelation zone above 50 °C (<1 min), we had to use a small frequency range (1 decade). In fact, for measurements done at a frequency lower than 10 rad/s, the time for measurement becomes too long; moreover, the reactive mixture can overflow from the plates at very high frequency (above 200 rad/s). Nevertheless, measurements could be carried on from 0.3 to 100 rad/s at 40 °C and from 3.16 to 100 rad/s at 50 °C.

Results

In a previous paper,[34] the kinetic study of the diglycidyl ether of 1,4-butanediol (DGEBD)/4,9-dioxa-1,12-dodecanediamine (4D) system was reported. As reported by many authors,[42−44] for a stoichiometric ratio equal to 1, the conversion of epoxy functions, x, obey the second-order autocatalytic model.

The knowledge of the kinetic equation (x as a function of time, t) (see Appendix A1) allows one to determine the theoretical extent of reaction, x_{gel}, at the gel point. The times corresponding to this value, x_{gel}, on the kinetics curves, which are the same as those obtained by the method of insoluble fractions, are compared to those found by viscosimetry (divergence of the viscosity, η, at the gel point) and viscoelasticity (crossover of the loss factor, tan δ, as a function of time at various frequencies).

As the gel point approaches, the mass-average molar mass, $\bar{M}_w$, diverges. This property was used to measure the theoretical value of x_{gel} in the case of equireactivity of the primary and secondary amine functions ($n = 1$),[45] or when the conversion of a primary amine to a

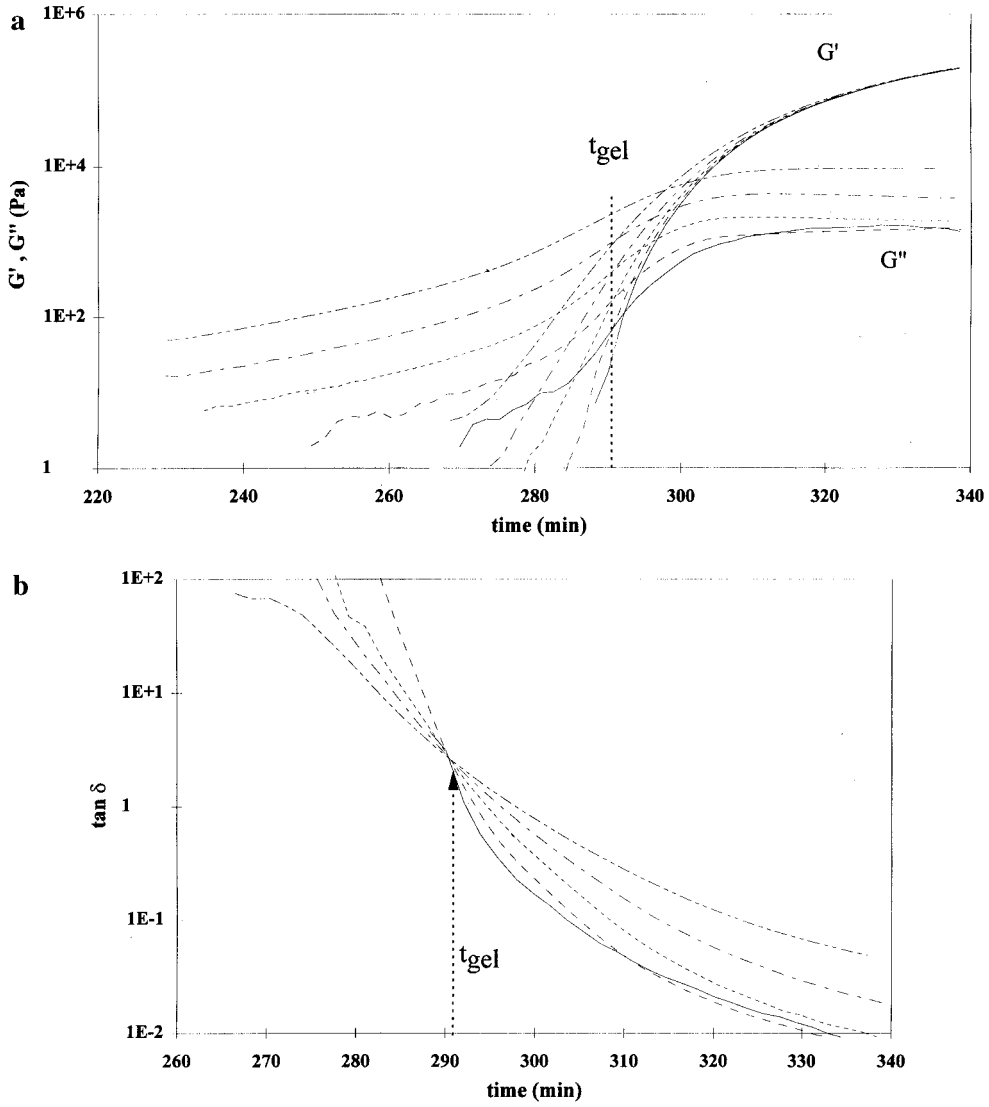

Figure 2. Experimental curves of storage shear modulus, G', and loss shear modulus, G'' (a), and of loss factor, tan δ (b), as function of reaction time, t, at 40 °C: (—) 1, (— — —) 3.16, (- - -) 10, (— - —) 31.6, and (— -- —) 100 rad/s.

secondary amine is associated with a substitution effect ($n \neq 1$).[46] In this last case, the following hypotheses are made: (a) all the groups of the same type have the same reactivity, (b) all the epoxy groups react independently, (c) all the amine groups are dependent on each other, and (d) there is no condensation product.

The third hypothesis (c) can be explained knowing that all the amine groups, A, of a monomer A_4 are of the primary type when no A site has reacted. An amine site, A, becomes a secondary site only if at least one amine A has reacted. Thus, the reaction probability of a site A taken at random depends only on the state (reacted or not) of the three other groups A of the monomer A_4. This probability is independent of the molecular conformation.

The expressions derived from the Macosko−Miller theory[46] are given in Appendix A2. Combining these results with the kinetic theory from Dušek,[47,48] it is possible to compute the theoretical extent of the reaction at the gel point. For $n = 1.1$, $x_{gel} = 0.5745$, which is slightly different than 0.577, the value obtained for the equireactivity of the primary and secondary amines ($n = 1$).[38,45] This theoretical value was used to determine the gel times from the kinetic curves.[34]

The dependence of the viscosity as a function of time is given in Figure 1 at 50 °C. A very rapid increase of the viscosity for times close to 140 min can be observed. The gel times are measured for a given viscosity ($\eta =$ 1000 Pa·s) and are reported in Table 2.

The evolution of G' (and G'') and of tan δ as a function of time at 40 °C are given in Figure 2, parts a and b, respectively. The gel times measured at crossover of tan δ vs time curves are also reported in Table 2. The tan δ values determined using this criterion can be found in Table 3.

According to Lairez et al.,[22] log G' vs time and log G'' vs time curves were fitted using a second-order polynomial equation near the gel point in order to take into account the fact that the measurements performed as a function of the frequency are not done at the same time (Figure 3). From these curves, log G' and log G'' are plotted as a function of log ω. A given time exists for which the log G' (or log G'') vs frequency curves display a linear dependence and have the same slope (Figure 4a at 40 °C). The exponent, Δ, is determined from the slope at this time. Figure 4b shows the critical behavior of G' vs ω and G'' vs ω for all the temperatures. The gel times found with this method are reported in Table 2, and the values of the exponent Δ are listed in Table 3.

Table 2 also gives the times for gelation calculated for $x = 0.5745$ from the kinetic equations. These gel times are very close to those obtained with the insoluble method (dissolution at different times in tetrahydrofu-

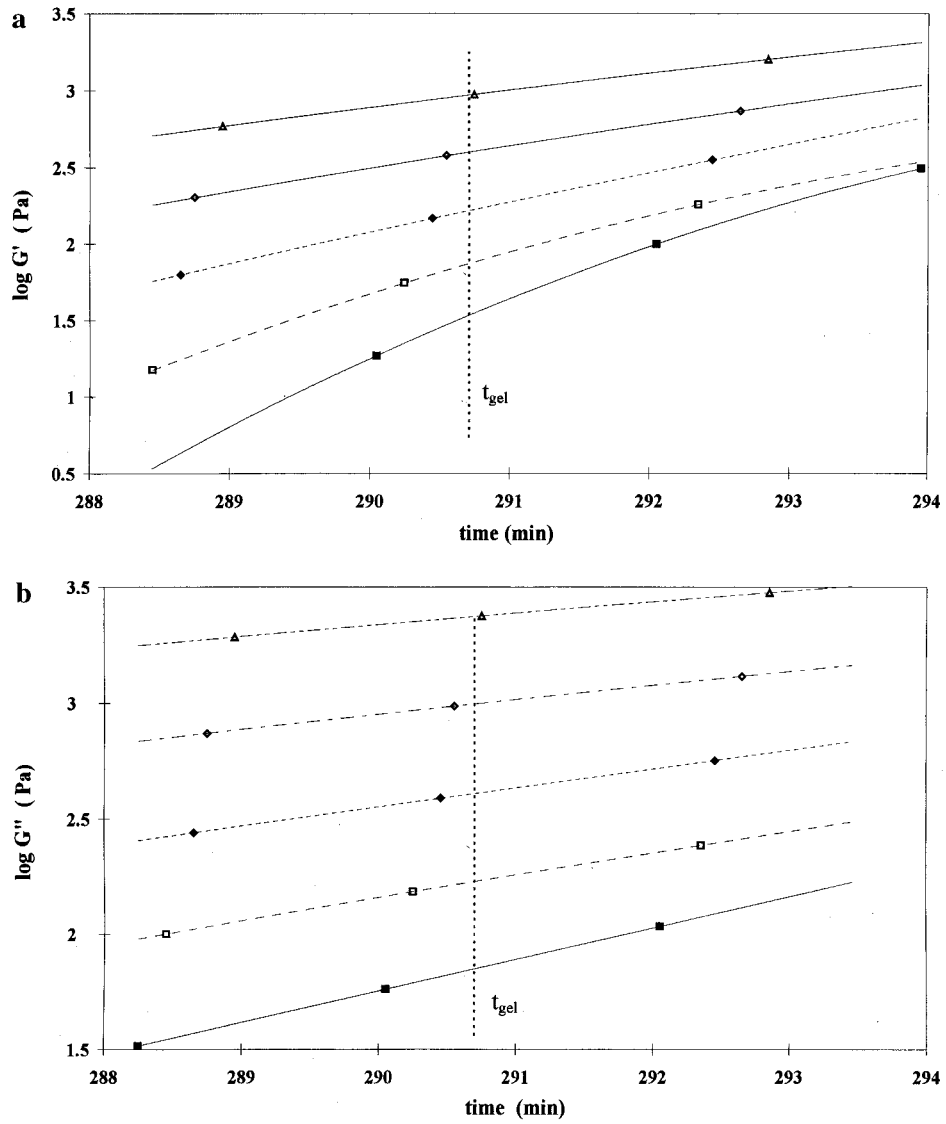

Figure 3. Second-order polynomial fitting of log G' vs reaction time (a) and log G'' vs reaction time (b) near the gel point at 40 °C: (■) 1, (□) 3.16, (◆) 10, (◇) 31.6, and (△) 100 rad/s.

ran, THF, and following the appearance of insoluble fractions). The times found from the different methods are very close to those obtained for $x = 0.5745$ (scattering around the mean value does not exceed 4%). This good agreement confirms the validity of the kinetic study and the second-order autocatalytic model which was retained.[34] As the conversion at the gel point is constant, the gel times obey an Arrhenius law as a function of temperature (Figure 5), with an activation energy of 60.3 kJ/mol. This value is very close to the activation energies of the kinetic constants K_0 and K_1 (59.4 and 58.3 kJ/mol, respectively).[34]

Table 3 gives the values of tan δ and of the exponent Δ' (the values of Δ' are derived from eq 20). The values of Δ and Δ' are similar, the discrepancy being <2%. This result confirms the validity of eq 20 and shows that the treatment used to get the exponent Δ is valid.

Discussion

Values of Δ as a Function of the Isothermal Temperature T_i. The exponent Δ decreases from 0.77 to 0.72 as the temperature increases from 40 to 50 °C. Above 50 °C, Δ remains fairly constant and equal to the average value, 0.70 ± 0.02. This value agrees well with those found by others authors for the diglycidyl ether of bisphenol A (DGEBA)/Jeffamine D400[18,19] and DGEBA/diethanolamine (DEA) systems.[20,21] In both cases, the isothermal temperatures, T_i, were higher than the maximum glass transition temperatures, $T_{g\infty}$ ($70 < T_i < 100$ °C and $T_{g\infty} = 35$ °C for DGEBA/D400; $T_i = 90$ °C and $T_{g\infty} = 70$ °C for DGEBA/DEA). As mentioned previously, the lower value found for DGEBA/4,4′-diaminodiphenyl sulfone (DDS)[22] might be due to the fact that the cure temperature, T_i (160 °C) is lower than $T_{g\infty}$ ($T_{g\infty} = 200$ °C) and that, in such a case, mobilities of macromolecular chains with long relaxation times occur.

To explain qualitatively the higher value of the exponent Δ at 40 °C, the dynamic mechanical response in the solid state of the fully cured network was performed in rectangular torsion. The cured schedule considered for this study consists of 20 h of polymerization at 40 °C, followed by a postcure of 1 h at 120 °C. The tan δ curves obtained at a given frequency as a function of temperature between −50 and 100 °C are given in Figure 6 for various fixed frequencies (from 1 to 100 rad/s). It is observed that the maximum of the main relaxation peak, α, associated with the glass transition temperature, occurs at −6 and 2 °C for frequencies of 1 and 100 rad/s, respectively. The $T_{g\infty}$ value measured by differential scanning calorimetry is −12 °C.[34] According to the frequency dependence effect,

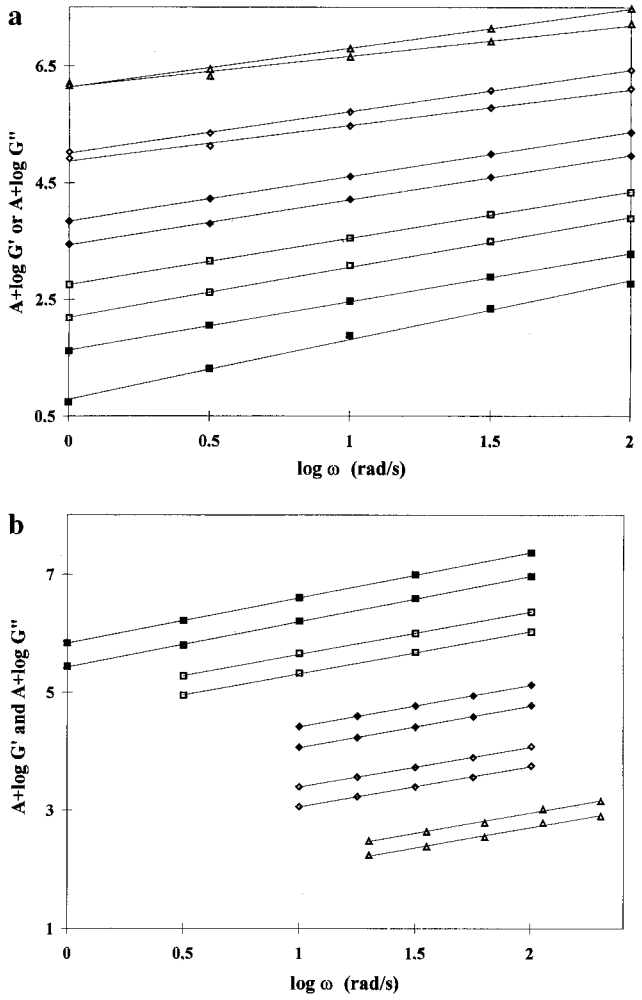

Figure 4. (a) Dependence of the storage and loss shear moduli, G' and G'', on the frequency, ω, near the gel point at 40 °C for different times of reaction: (■) ($A = 0$) 289, (□) ($A = 1$) 290, (◆) ($A = 2$) 290.7, (◇) ($A = 3$) 292, and (△) ($A = 4$) 293 min. (b) Dependence of G' and G'' on the frequency, ω, at the gel point for different temperatures of reaction: (■) ($A = 4$) 40, (□) ($A = 3$) 50, (◆) ($A = 2$) 55, (◇) ($A = 1$) 60, and (△) ($A = 0$) 70 °C.

Table 3. Critical Exponents as a Function of the Temperature

	T (°C)				
	40	50	55	60	70
tan δ	2.53	2.16	2.16	2.1	2
$\Delta' = 2\delta/\pi$	0.76	0.72	0.72	0.72	0.70
Δ	0.77	0.72	0.71	0.69	0.69
k	1.42	1.44	1.43	1.45	1.47
a^a	0.25	0.23	0.22	0.23	0.23
$z_0{}^a$	2.74	2.66	2.64	2.64	2.65
κ	0.23	0.25	0.24	0.25	0.22

[a] $z = z_0 + a \log \omega$.

the maximum of the tan δ peak measured at 100 rad/s appears at a temperature that is 14 °C higher than the DSC value. The difference between the isothermal cure temperature, T_i, and the maximum of the tan δ temperature is of the same order of magnitude as the width of the main relaxation zone, α, associated with the glass transition (Figure 6). Indeed, the width of the $H(\lambda)$ relaxation time distribution is connected to the half-height width, which is about 50 °C for 100 rad/s. As a consequence, the chain mobilities with relaxation times close to the observation time may occur at $T_i = 40$ °C, and these chains behave as in a vitreous state. Thus, the determination of the exponent Δ needs to be made

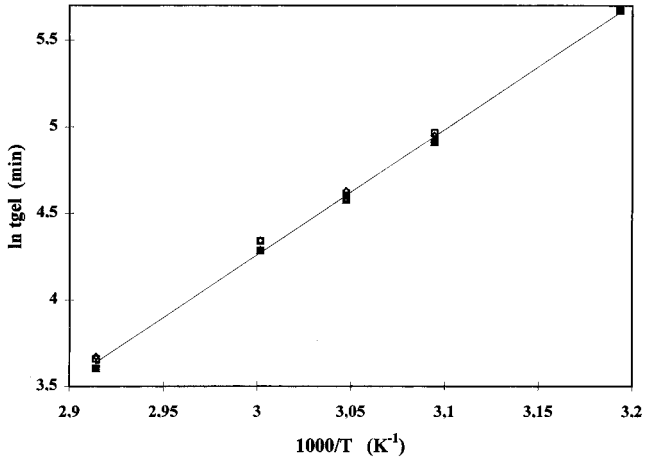

Figure 5. Arrhenius plot of the gelation phenomena (data from the various methods used to determine the gelation time): (□) $x = 0.5745$; (◇) $\eta = 1000$ Pa·s; (△) tan δ crossover; (■) $G' \propto G'' \propto \omega^{\Delta}$.

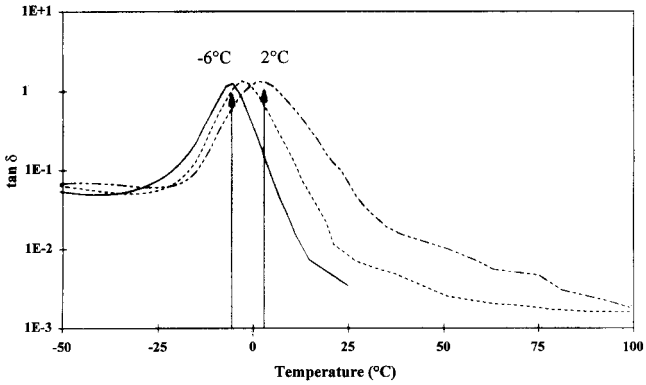

Figure 6. Loss factor, tan δ, as a function of the temperature for the fully cured network: (—) 1, (- - -) 10, and (— -- —) 100 rad/s.

at a temperature, T_i, which is much higher than the maximum glass transition temperature, $T_{g\infty}$ (i.e., the observation times, $1/\omega$, are much higher than the relaxation times, λ, in this case).

Evolution of $\eta(x)$ and $G'(x)$ near the Gel Point. The combination of the experimental results of viscosity, η, vs time and storage modulus, G', vs time, with the kinetic equation, x, vs time, gives η and G' as functions of the conversion, x, for all the temperatures (η vs x and G' vs x, respectively). Figure 7 displays the dependence of the viscosity, η, with conversion, x, obtained at 40, 50, 60, and 70 °C, while Figure 8 gives an example of the G' vs x curve at 40 °C. The lines represent the results obtained with eqs 9 (Figure 7) and 10 (Figure 8).

Figure 9 gives the curves log η vs $f(\log \epsilon)$, where $\epsilon = |x_{gel} - x|/x_{gel}$. A linear dependence of log η as a function of log ϵ can be noticed for ϵ from 1.6×10^{-3} to 0.5. This domain is broader than those generally considered in the literature ($0.015 < \epsilon < 0.5$), the inferior limit being nearer to zero.[28] In addition, it is observed that, in the literature, ϵ is often expressed as a function of the reaction time, t, instead of the conversion, x.

The critical exponents obtained from a regression at various temperatures are reported in Table 3. The slight increase of k which could be observed between 40 and 70 °C does not seem significant, and this exponent can be considered a constant. Its value (1.44 ± 0.03) is in good agreement with those found for the DGEBA/DEA system (1.4 ± 0.2)[16,20,21] and for the DGEBA/D400 system (1.3 ± 0.2).[19] This value is very close to that from the Rouse model.

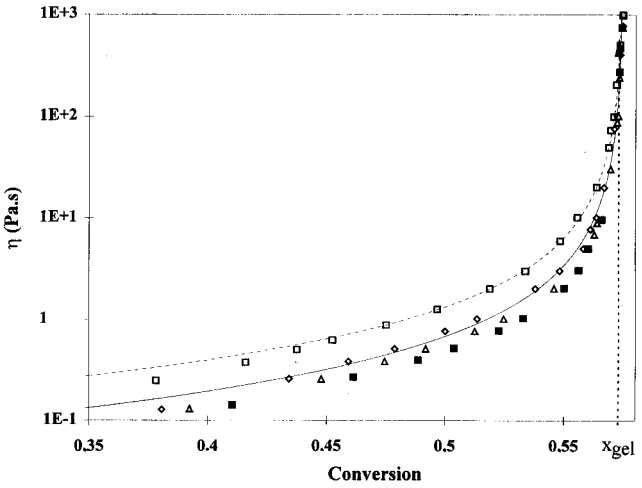

Figure 7. Viscosity, η, as a function of the extent of the reaction, x (the lines represent the theoretical curves obtained at 40 and 50 °C using eq 9): (□) 40, (◇) 50, (△) 60, and (■) 70 °C.

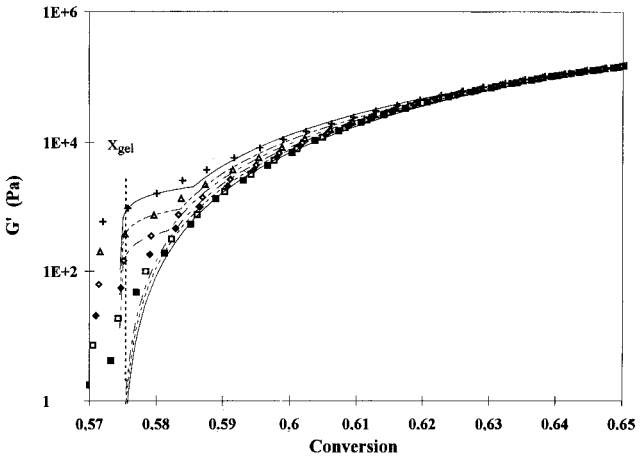

Figure 8. Storage shear modulus, G', as a function of the extent of reaction, x, at 40 °C (the lines represent the theoretical curves obtained using eq 10): (■) 0.31, (□) 1, (◆) 3.16, (◆) 10, (△) 31.6, and (+) 100 rad/s.

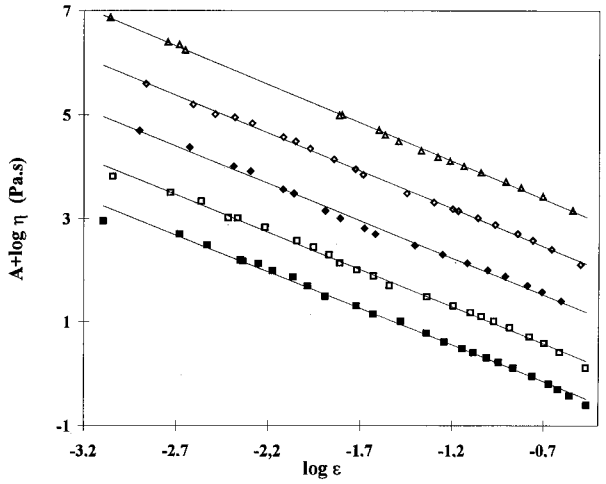

Figure 9. Dependence of the viscosity, η, as a function of log ϵ ($\epsilon = |x_{gel} - x|/x_{gel}$)SPCLN (■) ($A = 0$) 40, (□) ($A = 1$) 50, (◆) ($A = 2$) 55, (◇) ($A = 3$) 60, and (△) ($A = 4$) 70 °C.

Figure 10 shows the log G' vs log ϵ curves at 40 °C. Two domains of linear dependence are observed, at least for higher frequencies. For the lower frequencies, it is not so clear, because the time for which the storage modulus, G', increases is very close to the gel point when the frequency is reduced. The existence of the first zone might only be due to the fact that the frequency of measurement is not zero. Yu et al.[25] observed both zones for their experiments on gelatin and tetraethoxysilane gelations at high frequencies (ω from 650 to 39 000 rad/s). For the high temperatures, the rapid occurrence of a crossing for the tan δ through the gel zone does not give us enough significant points to observe the same behavior. In the second domain, the exponent z varies with frequency. Figure 11 shows that the z vs log ω curves are straight lines ($z = z_0 + a \log \omega$). As expected, the exponent z is reduced as the frequency increases. Indeed, the modulus is constant at the rubbery plateau whatever the frequency is.

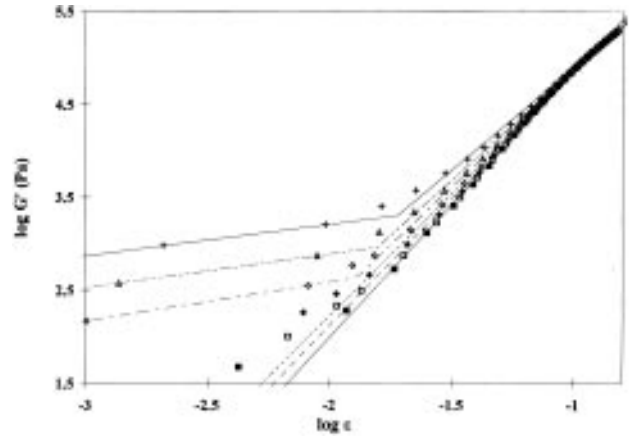

Figure 10. Dependence of log G' on log ϵ ($\epsilon = |x_{gel} - x|/x_{gel}$) at $T = 40$ °C: (■) 0.31, (□) 1, (◆) 3.16, (◇) 10, (△) 31.6, and (+) 100 rad/s.

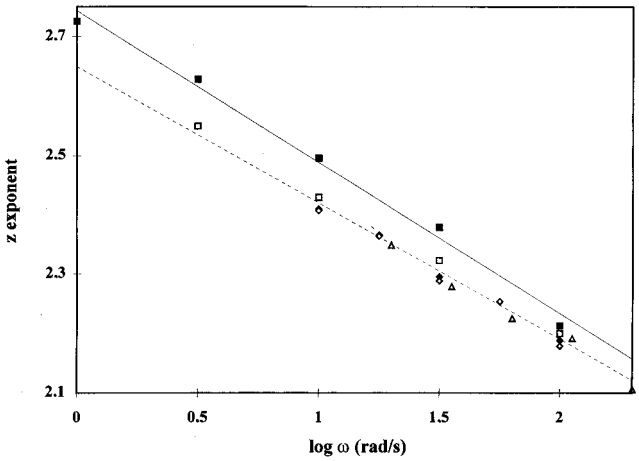

Figure 11. Dependence of the exponent z on the frequency, ω: (■) 40, (□) 50, (◆) 55, (◇) 60, and (△) 70 °C.

In Table 3 are reported the values of z_0 and a (z_0 is the value of z corresponding to $\omega = 1$ rad/s). A decrease of z_0 between 40 and 50 °C can be observed. This behavior can be related to that previously observed for the exponent Δ. From 50 to 70 °C, z_0 remains constant, with a mean value of 2.65 ± 0.02. This behavior agrees well with the data given by the Rouse model (2.67) and those found for the DGEBA/DEA system[20] (2.80 ± 0.2). It should be noted that the frequency used in this case was 1 rad/s.

The log G^* vs time curves were fitted in the vicinity of the gel point using a second-order polynomial equation. Thus, the values of $\partial(\log G^*)/\partial t$ for $t = t_{gel}$ were calculated and are plotted in Figure 12 as a function of the frequency for all the temperatures. The exponents, κ, obtained from the regression (see eq 33) are reported in Table 3. It is observed that this exponent is slightly dependent on the temperature. Its mean value ($0.24 \pm$

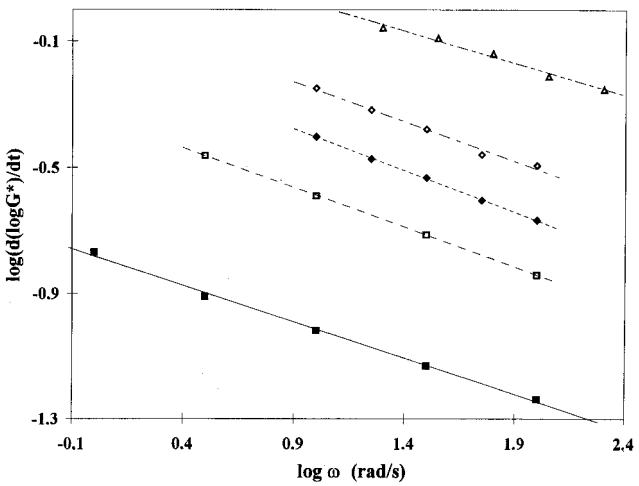

Figure 12. log(∂ log $G^*/\partial t$) as a function of the logarithm of the frequency, ω: (■) 40, (□) 50, (◆) 55, (◇) 60, and (△) 70 °C.

Table 4. Comparison of the Values of the Critical Exponents

	exponents			
	Δ	k	z_0	κ
exptl mean values	0.70 ± 0.02	1.44 ± 0.03	2.65 ± 0.02	0.24 ± 0.02
calcd values	0.65 ± 0.02[a]	1.25 ± 0.20[b]	2.9 ± 0.3[c]	
Rouse model	0.67	1.33	2.67	0.25

[a] $\Delta'' = z_0/(z_0 + k)$. [b] $k' = (1 - \Delta)/\kappa$. [c] $z' = \delta/\kappa$.

0.02) well agrees with the one predicted by the Rouse model (0.25). From the mean values of the exponents Δ, k, z_0, and κ, the exponents Δ'', k', and z' can be computed from eqs 24 and 35. The results reported in Table 4 are closed to those found in the Rouse percolation model.

Conclusion

We have presented a determination of the times for gelation using different techniques and of the exponents k, z, Δ, and κ for a flexible (low-T_g) epoxy−amine system, the DGEBD/4D system, as a function of the temperature near the gel point. The mechanical properties were studied as a function of the extent of reaction and not only as a function of time, as is often done in the literature.

The results obtained lead to the following observations:

(i) The gel times obtained from different experimental and analysis methods (for $x_{gel} = 0.5745$; for a given viscosity $\eta = 1000$ Pa·s; crossover of the tan δ vs $f(t)$ curves; G' and $G'' \propto \omega^{\Delta}$) are identical according to the accuracy of the measurements. This phenomenon confirms the validity of the kinetic study and of the second-order autocatalytic model.

(ii) The exponent Δ is quite constant from 50 to 70 °C, and its value is close to that of the percolation model. The decrease observed between 40 and 50 °C can be related to the molecular mobilities. In fact, according to the width of the relaxation time spectrum, the relaxation times should be of the same order of magnitude as the observation times.

(iii) A linear dependence of the logarithm of the viscosity, η, and the logarithm of the storage shear modulus, G', with the log ϵ is observed corresponding to the behavior provided by equations $\eta \propto \epsilon^{-k}$ and $G \propto \epsilon^{z}$ in a large domain. Moreover, a second domain observed at higher frequencies and lower temperatures on log G' curves proceeds from the fact that the G' measurement is not performed at zero frequency.

(iv) The values found for the exponents k, z_0, and κ are very close to those predicted by the percolation theory with the Rouse model. The same behavior is reported for Δ'' calculated from k and z_0 and for k' and z' obtained from Δ and κ.

Thus, we can conclude that the reactional medium of the DGEBD/4D system can be considered as a polymolecular system which can be described by the percolation model with chains obeying the Rouse model from 40 to 70 °C, i.e., from $T_{g\infty}$ + 50 °C and $T_{g\infty}$ + 80 °C, respectively.

Appendix 1: Kinetic Equation for the DGEBD/4D System[34]

The kinetic equation for the DGEBD/4D system is given as

$$dx/dt = (1 - x)(K_0 + K_1x)[2\alpha(1 - n) + n\alpha^{n/2}]/(2 - n)$$

$$d\alpha/dt = -2\alpha(1 - x)(K_0 + K_1x) \qquad \text{(A1-1)}$$

with

$$x = (e_0 - e)/e_0$$

$$\alpha = a_1/e_0$$

e = concentration of epoxy functions (e_0 at time $t = 0$)

a_1 = concentration of primary amine functions ($a_{10} = a_0$ at time $t = 0$)

$n = 1.1$ = reactivity ratio between secondary and primary amines

$$K_0 = 2.87 \times 10^6 \exp(-59.4 \times 10^3/RT)\ (\text{min}^{-1})$$

$$K_1 = 1.04 \times 10^8 \exp(-58.5 \times 10^3/RT)\ (\text{min}^{-1}) \qquad \text{(A1-2)}$$

Appendix 2: Calculation of the Theoretical Extent of Reaction, x_{gel}

In the case of the first-order substitution effect, the mass-average molar mass, M_w, for $A_4 + E_2$ (amine A_4 of functionality 4 and epoxy E_2 of functionality 2) can be obtained by

$$M_w = \{[1 + x(4x - X + 1)](M_{A_4})^2 + 2[1 + x(X - 1)](M_{E_2})^2 + 8xM_{A_4}M_{E_2}\}/\{(M_{A_4} + 2M_{E_2})[1 - x(X - 1)]\} \qquad \text{(A2-1)}$$

with

$$\alpha_i = A_{4,i}/A_0$$

$$x = (^1/_4)\sum_i \alpha_i \qquad 0 \le i \le 4$$

$$X = (^1/_4x)\sum_{i^2} \alpha_i \qquad 0 \le i \le 4$$

where M_{A_4} is the molar mass of the amine, M_{E_2} is the molar mass of the epoxy, $A_{4,i}$ is the number of A_4 moles

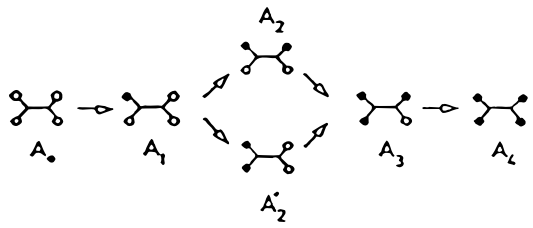

Figure 13. Kinetics of the epoxy−amine systems. k_1, kinetic constant of the primary amine/secondary amine reaction; k_2, kinetic constant of the secondary amine/tertiary amine reaction; $A_{4,i}$, number of A_4 moles for which i sites have reacted.

for which i amine groups have reacted, and A_0 is the initial number of amine functions.
Thus, x_{gel} is given by the following equation:

$$1 - x(X - 1) = 0 \qquad \text{(A2-2)}$$

The resolution of this equation requires knowledge of the parameters α_i. Their values were determined from the kinetic theory proposed by Dušek[47,48] (Figure 13):

$$n = k_2/k_1 p = 2/(2 - n)q = (2 + n)/2$$

$$\alpha_0 = A_{4,0}/A_0$$

$$\alpha_1 = A_{4,1}/A_0 = 2p(\alpha_0{}^q - \alpha_0)$$

$$\alpha_2 = A_{4,2}/A_0 = \alpha'_2 + \alpha''_2 = p^2(-2\alpha_0{}^q + \alpha_0 + \alpha_0{}^{n/2}) - 2p\alpha_0{}^q + np\alpha_0 + 2\alpha_0{}^{1/2} \qquad \text{(A2-3)}$$

$$\alpha_3 = A_{4,3}/A_0 = p_2[(n + 2)\alpha_0{}^q - n\alpha_0 - (2 - n)\alpha_0{}^{1/2} - 2\alpha_0{}^{n/2} + (2 - n)\alpha_0{}^{n/4}]$$

$$\alpha_4 = A_{4,4}/A_0 = p_2[-n\alpha_0{}^q + (n/2)^2\alpha_0 + (n/p)\alpha_0{}^{1/2} + (2 - n)\alpha_0{}^{n/4} + 1/p^2]$$

$$x = 1 - [(1 - n)\alpha_0{}^{1/2} + \alpha_0{}^{n/4})]/(2 - n) \qquad \text{(A2-4)}$$

Equations A1-1 and A1-2 lead to x as a function of time for a given temperature. The numerical resolution of eq A2-4 gives α_0 as a function of time. Then we can calculate the α_i vs time parameters ($1 \le i \le 4$) and finally obtain x_{gel} by solving eq A2-2.

References and Notes

(1) Alexander, S.; Orbach, R. *J. Phys. (Paris) Lett.* **1982**, *43*, L625.
(2) Muthukumar, M. *J. Chem. Phys.* **1985**, *83*, 3162.
(3) Muthukumar, M. *Macromolecules* **1989**, *22*, 4656.
(4) Hess, W.; Vilgis, T. A.; Winter, H. H. *Macromolecules* **1988**, *21*, 2536.
(5) Rubinstein, M.; Colby, R.; Gillmor, J. R. *Polym. Prepr., Am. Chem. Soc. Div. Polym. Chem.* **1989**, *30*, 81.
(6) Martin, J. E.; Adolf, D.; Wilcoxon, J. P. *Phys. Rev.* **1989**, *A39*, 1325.
(7) Durand, D.; Delsanti, M.; Adam, M.; Luck, T. M. *Europhys. Lett.* **1987**, *3*, 277.
(8) Adolf, D.; Hance, B.; Martin, J. E. *Macromolecules* **1993**, *26*, 2754.
(9) Chambon, F.; Winter, H. H. *Polym. Bull.* **1985**, *13*, 499.
(10) Chambon, F.; Winter, H. H. *J. Rheol.* **1986**, *30*, 367.
(11) Chambon, F.; Winter, H. H. *J. Rheol.* **1987**, *31*, 683.
(12) Scanlan, J. C.; Winter, H. H. *Makromol. Chem., Macromol. Symp.* **1991**, *45*, 11.
(13) Scanlan, J. C.; Winter, H. H. *Macromolecules* **1991**, *24*, 47.
(14) Izuka, A.; Winter, H. H.; Hashimoto, T. *Macromolecules* **1992**, *25*, 2422.
(15) Izuka, A.; Winter, H. H.; Hashimoto, T. *Macromolecules* **1994**, *27*, 6883.
(16) Martin, J. E.; Adolf, D.; Wilcoxon, J. P. *Phys. Rev. Lett.* **1988**, *61*, 2620.
(17) Hodgson, D. F.; Amis, E. J. *Macromolecules* **1990**, *23*, 2512.
(18) Matjeka, L. *Polym. Bull.* **1991**, *26*, 109.
(19) Miaoling, L. H.; Williams, J. G. *Macromolecules* **1994**, *27*, 7423.
(20) Adolf, D.; Martin, J. E. *Macromolecules* **1990**, *23*, 3700.
(21) Adolf, D.; Martin, J. E.; Wilcoxon, J. P. *Macromolecules* **1990**, *23*, 527.
(22) Lairez, D.; Adam, M.; Emery, J. R.; Durand, D. *Macromolecules* **1992**, *25*, 286.
(23) Takahashi, M.; Yokohama, K.; Musada, T.; Takigawa, T. *J. Chem. Phys.* **1994**, *101*, 798.
(24) Koike, A.; Nemoto, N.; Takahashi, M.; Osaki, K. *Polymer* **1994**, *35*, 3005.
(25) Surivet, F.; Lam, T. M.; Pascault, J. P.; Pham, Q. T. *Macromolecules* **1992**, *25*, 4309.
(26) Yu, Q.; Amis, E. J. *Makromol. Chem., Macromol. Symp.* **1993**, *76*, 193.
(27) Hsu, S.; Jamieson, A. M. *Polymer* **1993**, *34*, 2602.
(28) Djabourov, M. *Polym. Int.* **1991**, *25*, 135.
(29) de Gennes, P. G. *C. R. Acad. Sci. Ser. B* **1978**, *286*, 131.
(30) de Gennes, P. G. *Scaling Concepts in Polymer Physics*; Cornell University Press: Ithaca, NY, 1979.
(31) Derrida, B.; Stauffer, D.; Hermann, H. J.; Vannimenus, J. J. *Phys. (Paris) Lett.* **1983**, *44*, L701; **1984**, *45*, L913.
(32) Hermann, H. J.; Derrida, B.; Vannimenus, J. *Phys. Rev.* **1984**, *B30*, 4080.
(33) Stauffer, D. *Introduction to Percolation Theory*; Taylor and Francis: London, 1985.
(34) Eloundou, J. P.; Fève, M.; Harran, D.; Pascault, J. P. *Angew. Makromol. Chem.* **1995**, *220*, 13.
(35) Stauffer, D.; Coniglio, A.; Adam, M. *Adv. Polym. Sci.* **1982**, *44*, 103.
(36) Ferry, J. D. *Viscoelastic Properties of Polymers*, 3rd ed.; Wiley: New York, 1980.
(37) Hodgson, D. F.; Amis, E. J. *Phys. Rev.* A **1990**, *41*, 1182.
(38) Flory, J. P. *Principles of Polymer Chemistry*; Cornell Universty Press: Ithaca, NY, 1953.
(39) Graessley, W. W. *Macromolecules* **1975**, *8*, 186.
(40) Winter, H. H. *Prog. Colloid. Polym. Sci.* **1987**, *75*, 104.
(41) Kanai, H.; Navarrette, R. C.; Macosko, C. W.; Scriver, L. E. *Rheol. Acta* **1992**, *31*, 333.
(42) Serier, A.; Pascault, J. P.; My, L. T. *J. Polym. Sci., Polym. Chem. Ed.* **1991**, *29*, 209.
(43) Riccardi, C. C.; Williams, R. J. J. *J. Appl. Polym. Sci.* **1986**, *32*, 3445.
(44) Cuadrado, T. R.; MacGregor, J. F.; Hamielec, A. E. *J. Appl. Polym. Sci.* **1990**, *40*, 867.
(45) Macosko, C. W.; Miller, D. R. *Macromolecules* **1976**, *9*, 206.
(46) Miller, D. R.; Macosko, C. W. *Macromolecules* **1980**, *13*, 1063.
(47) Dušek, K.; Ilavzky, M.; Lunak, S. *J. Polym. Sci., Polym. Symp.* **1975**, *53*, 29.
(48) Dušek, K. *Adv. Polym. Sci.* **1986**, *78*, 1.

MA960287D